

## Electron Microscopy Study on the Effect of Si<sub>3</sub>N<sub>4</sub> addition to B<sub>4</sub>C-SiC-Al Composites

Pinar KAYA<sup>1</sup>, Ayse Kalem tas<sup>2</sup>, Gursoy Arslan<sup>1</sup>, Ferhat KARA<sup>1</sup>, Servet Turan<sup>1</sup>

<sup>1</sup> Department of Material Science & Engineering, Anadolu University, Eskisehir, Turkey

<sup>2</sup> Department of Material Science & Engineering, Bursa Technical University, Bursa, Turkey

Monolithic ceramics such as Si<sub>3</sub>N<sub>4</sub>, AlN and SiC possess a good combination of properties including high thermal conductivity, high electrical resistivity, high hardness, high elastic modulus and high strength due to their strong covalent bonding however they are inherently brittle. The use of AlN based ceramic components for structural, electrical and electronic applications is increasing rapidly, but the difficulties in machining, the low reliability and expensive production tools and raw materials have hindered the in cost-effective use of these materials [1]. Ceramic-metal composites have a wide range of applications such as materials for energy technology, automotive industry and military applications [2]. Several processing techniques, including powder metallurgy, casting, infiltration, directed metal oxidation, etc., have been developed to produce ceramic-metal composites. Pressureless melt infiltration is generally considered to be a more attractive technique to produce ceramic-metal composites due to its cost effectiveness and easiness when compared to more conventional methods such as casting and powder metallurgy [3]. Moreover, the near net shape capability of pressureless melt infiltration process with the combination of using an economical  $\alpha$ -Si<sub>3</sub>N<sub>4</sub> starting powder instead of expensive sub-micron AlN, make the AlN based products more better candidates for the applications [4]. For this purpose, porous pellets were produced by using SiC and B<sub>4</sub>C powder mixture prepared with and without using Si<sub>3</sub>N<sub>4</sub> powder, which were then pressureless melt infiltrated with a 2024 Al alloy at 1100°C for 1 hour in an Ar gas atmosphere. These composites were characterized by employing XRD, SEM and TEM techniques. Detailed TEM studies on the specimen were carried out by using STEM imaging, STEM-EDX, EFTEM and EELS techniques.

Phase analysis of the SiC-B<sub>4</sub>C-Al composites revealed that a significant amount of hygroscopic Al<sub>4</sub>C<sub>3</sub> phase was formed besides the main reaction products of Al<sub>3</sub>BC and Si. Si<sub>3</sub>N<sub>4</sub> powder was added to SiC-B<sub>4</sub>C powder batches, to suppress the formation of Al<sub>4</sub>C<sub>3</sub> phase via in-situ reactions during the infiltration process. XRD analysis confirmed the incorporation of Si<sub>3</sub>N<sub>4</sub> significantly reduced the formation of the Al<sub>4</sub>C<sub>3</sub> phase and resulted in the formation of phases such as AlN, SiC and Si (Fig. 1). SEM investigations of these composites revealed that the microstructure is very fine (<1  $\mu$ m) (Fig. 2a). Since ceramic-metal interface characterization and its detailed elemental analyses could not be carried out by SEM-related characterization techniques. The ceramic-metal interfaces, as well as the size and distribution of the reaction products, were investigated by using TEM techniques. Both STEM-HAADF and BF images confirmed the SEM results in terms of the size of the reaction products (Fig. 2b and 2c). Furthermore, addition of Si<sub>3</sub>N<sub>4</sub> results in the formation of AlN and free metallic Si as well as the suppression of Al<sub>4</sub>C<sub>3</sub> phase in the composite system which is clearly seen from overlay EFTEM map (Fig. 3).

### References

- [1] Janssen R., Scheppokat S., and Claussen N., J. Eur. Cer. Soc., 28 (2008), 1369–1379.
- [2] Aghajanian M. K., *et al.*, J. Mater. Sci., 26 (1991) 447
- [3] Akhtar F., Guo S., Trans. Nonferrous Met. Soc. China 16, (2006), 629-632
- [4] Kalem tas, Ayse, *et al.*, Transactions of Nonferrous Metals Society of China 23 (2013), 1304-1313.

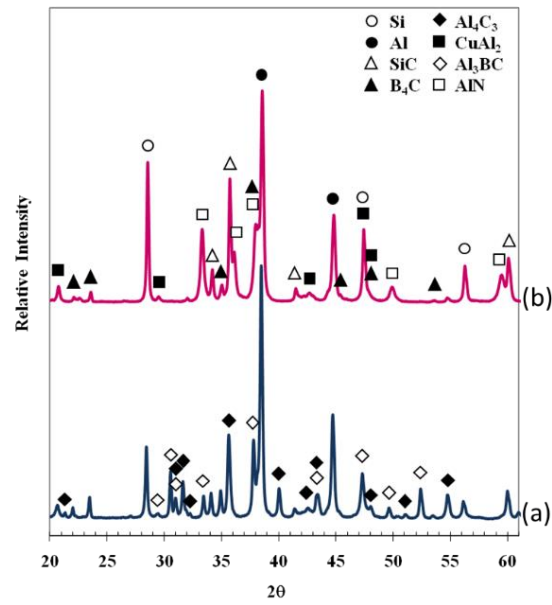


Figure 1. XRD pattern of (a) B<sub>4</sub>C-SiC-Al (b) Si<sub>3</sub>N<sub>4</sub>-B<sub>4</sub>C-SiC-Al composites.

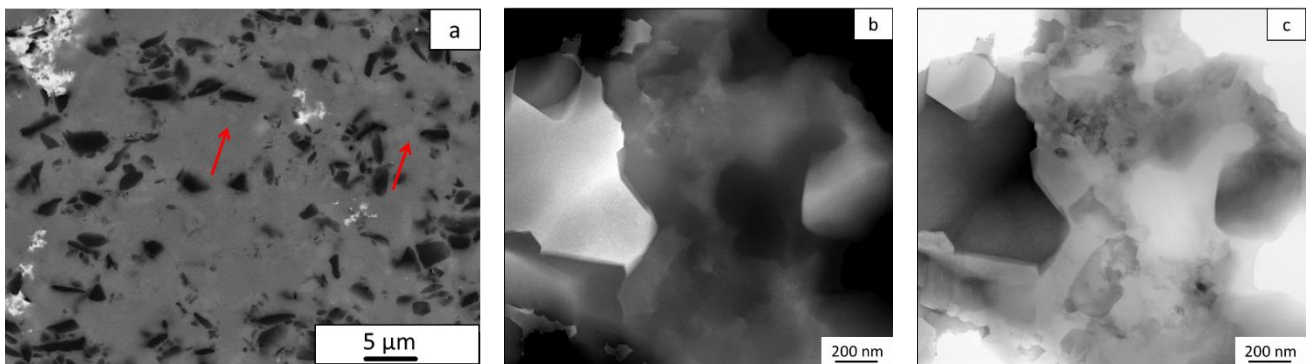


Figure 2. (a) SEM-BSE (b) STEM-HAADF (c) STEM-BF images of Si<sub>3</sub>N<sub>4</sub>-B<sub>4</sub>C-SiC-Al composite.

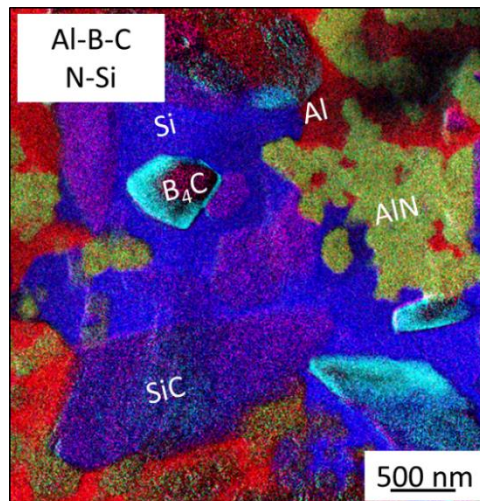


Figure 3. EFTEM three window overlay maps of the Si<sub>3</sub>N<sub>4</sub>-B<sub>4</sub>C-SiC-Al composite